Frequently amplified c-MET and STAT3 signalling drives malignant peripheral nerve sheath tumour (MPNST) cell migration, invasion and tumour formation

Elham Marzban Rad, Laura Elizabeth Thomas, Kayleigh Margaret Dodd, Meena Upadhyaya and Andrew Robert Tee*

Institute of Cancer and Genetics, Cardiff University, Heath Park, Cardiff, Wales, CF14 4XN, UK.

***Corresponding author:** Dr. Andrew R. Tee, Institute of Cancer and Genetics, Cardiff University, Cancer Genetics Building, 1st Floor, Heath Park, Cardiff, CF14 4XN, UK.

Telephone number: +44 2920 687856, e-mail address: teea@cardiff.ac.uk

Short title: c-MET and STAT3 drives MPNSTs malignancy

Keywords: c-MET; MPNST; NF1; STAT3; mTOR

Abbreviations: c-MET, c-MET Proto-oncogene product; DMEM, Dulbecco's Modified Eagle Medium EGF-R; 5,15-DPP, 5,15-diphenylporphyrin; Epidermal Growth Factor Receptor; FBS, Fetal Bovine Serum; HGF, Hepatocyte Growth Factor; IL-6, Interleukin-6; IL-R, Interleukin Receptor; JAK2, Janus kinase 2; MPNST, Malignant Peripheral Nerve Sheath Tumour; mTORC1, mammalian target of rapamycin complex 1; NF1, Neurofibromatosis Type 1; PDGF, Platelet-derived growth factor; PDGF-R, Platelet-derived growth factor Receptor; PI3K, Phosphoinositide 3-kinase; PTEN, Phosphatase and tensin homolog; SH2, Src Homology 2; STAT3, Signal transducer and activator of transcription 3

Abstract

Therapeutic options are currently limited for Neurofibromatosis type 1 (NF1) malignant peripheral nerve sheath tumours (MPNSTs). MPNSTs are characteristically aggressive and are the major cause of morbidity in NF1 patients. Clinical trials for NF1 with single drug agents have so far been ineffective, which may be due to the high level of intra-tumoural molecular heterogeneity of MPNSTs. To explore different cell migratory and invasive signalling properties within NF1-MPNSTs, and to test multi-drug therapeutic options, we utilised four MPNST cell lines with marked differences in the levels of c-MET expression, ST8814, S462, S1844.1 and S1507.2. We show that the cellular migration and invasion of ST8814 cells, which have amplified signal transduction through HGF/c-MET/STAT3, were

highly sensitive to c-MET inhibitors, SU11274 and PF-4217903. In contrast, cell migration and invasion of S462 cells was unaffected by c-MET inhibition, which was attributed to lower levels of c-MET expression and a reduced c-MET/STAT3 response to HGF stimulation. Of importance, migration of all four NF1-MPNST cell lines, ST8814 and S462, S1844.1 and S1507.2 were highly sensitive to a panel of JAK2/STAT3 inhibitors, Cucurbitacin-I, 5,15-diphenylporphyrin (5,15-DPP) and FLLL31. Furthermore, STAT3 knockdown prevented wound healing and tumour formation in soft agar within all NF1-MPNST cell lines analysed, revealing that STAT3 is necessary for tumourgenesis in multiple NF1-MPNST cell lines with varying signalling profiles. This research reveals that STAT3 frequently promotes cell migration, invasion, proliferation and tumour formation within the heterogeneous NF1-MPNST population. This work implies that inhibition of signal transduction through STAT3 could be a viable therapeutic strategy to treat NF1-MPNSTs.

1. Introduction

Neurofibromatosis type 1 (NF1), is an autosomal dominant tumour predisposition syndrome affecting approximately 1 in 3500 individuals (Upadhyaya, 2010). The *NF1* gene (17q11.2), encodes neurofibromin, a 2818 amino acid protein, which is highly expressed in the brain and central nervous system. NF1 is clinically characterised by hyperpigmentary abnormalities of the skin (café-au-lait macules and inguinal/axillary freckling), iris hamartomas (Lisch nodules) and the growth of benign peripheral nerve sheath tumours (neurofibromas) in the skin (Ferner et al., 2007; Upadhyaya, 2010). Neurofibromin functions as a tumour suppressor by acting as a GTPase-activating protein (GAP) towards the small G-protein Ras (Arun and Gutmann, 2004; Bennett et al., 2009; Katz et al., 2009; Scheffzek et al., 1998). Consequently, inactivating mutations to *NF1* lead to increased signal transduction through Ras to promote uncontrolled cell growth and tumourigenesis (Klose et al., 1998; Thomas et al., 2012).

Malignant peripheral nerve sheath tumours (MPNSTs) are the main cause of morbidity in NF1 (Bennett et al., 2009; Upadhyaya, 2011; Walker et al., 2006). MPNSTs usually arise from pre-existing plexiform neurofibromas, however, MPNSTs are also known to occur sporadically (King et al., 2000). MPNSTs represent 10% of all soft tissue sarcomas with 50% occurring in association with NF1. The lifetime risk of developing sporadic MPNST is 0.001%, compared to 5-13% for NF1 patients (Ducatman et al., 1986). NF1-MPNSTs usually develop in the second or third decade of life (Ellison et al., 2005). While sporadic MPNSTs often occur much later in life. Therapeutic options are currently inadequate for treating NF1-MPNSTs and associated tumours (Katz et al., 2009). The primary therapeutic procedure is complete surgical excision with clear margins, however the local recurrence of NF1-MPNSTs

is high and ranges from 32% to 65% (Porter et al., 2009). The risk factors for development of NF1-MPNSTs include the presence of internal plexiform neurofibromas (Tucker et al., 2005), high tumour burden (Mautner et al., 2008), microdeletion of *NF1* locus (De Raedt et al., 2003) and prior radiation treatment (Meadows and Silber, 1985).

Although multiple receptor tyrosine kinases are known to be amplified in MPNSTs, clinical trials that target receptor tyrosine kinases for MPNSTs have been challenging (Korf et al., 2012). For instance, a phase II trial employing epithelial growth factor receptor (EGFR) inhibitor, erlotinib, was not successful (Albritton et al., 2006). Subsequently, a phase II clinical trial was initiated employing the RAF kinase and receptor tyrosine kinase inhibitor, Sorafenib, which was also ineffective (Maki et al., 2009). Furthermore, no clear response was observed in phase II clinical trials with receptor tyrosine kinase inhibitors, Gleevec (Chugh et al., 2009) and Dasatinib (Schuetze et al., 2010). It is probable that the heterogeneity of MPNSTs (Mantripragada et al., 2008; Mawrin et al., 2002; Nielsen et al., 1999; Thomas et al., 2012; Upadhyaya et al., 2006) is an underlying cause for the lack of success in these clinical trials. For instance, analysis of *NF1*, *TP53*, *RB1*, *PTEN*, and *CDKN2A* gene markers linked to MPNST tumour progression for loss of heterozygosity, have shown a high level of intra-tumoural molecular heterogeneity (Thomas et al., 2012). In view of this, it is unlikely that the use of a single drug agent would sufficiently impact the growth, malignancy and survival of all the varied tumour sub-types that constitutes the whole MPNST population. A more pragmatic approach may be to utilise a combination of drugs that collectively target overlapping and commonly deregulated molecular pathways that drive the malignant phenotype of multiple MPNSTs.

Much progress has been made in determining the molecular pathophysiology of MPNSTs. High-throughput whole genome analysis with microarrays has provided the most insight into new therapeutic options by revealing patterns of molecular signatures common in MPNSTs that are not present in benign neurofibromas, i.e., copy number variations and gene expression changes (Beert et al., 2011; Brekke et al., 2010, 2009; Bridge et al., 2004; Chai et al., 2010; Holtkamp et al., 2004; Kresse et al., 2008; Largaespada and Ratner, 2013; Lothe et al., 1996; Luscan et al., 2013; Mantripragada et al., 2009, 2008; Miller et al., 2006; Mo et al., 2013; Pemov et al., 2010; Rahrmann et al., 2013; Schuetze et al., 2010; Shen et al., 2007; Storlazzi et al., 2006; Subramanian et al., 2010; Upadhyaya et al., 2012; Watson et al., 2013, 2004). We previously determined that the *HGF*, *c-MET*, and *PDGFRA* genes were frequently amplified in MPNSTs (Mantripragada et al., 2008). The proto oncogene *c-MET* encodes the C-MET Proto-oncogene product (c-MET) transmembrane receptor tyrosine kinase for its sole ligand, hepatocyte growth factor (HGF, also known as hepatopoietin and scatter factor) (Bottaro et al., 1991; Naldini et al., 1991). HGF/c-MET

signalling is known to drive cellular proliferation, anti-apoptotic responses and metastasis (Birchmeier et al., 2003). It is known that HGF/c-MET signalling reduces cell-to-cell adhesion, heightens cell motility and increases proteolytic activity of matrix metalloproteases, which overall promotes tumour cell invasiveness (Krasnoselsky et al., 1994).

To identify potential therapeutic options for treating NF1-MPNSTs with varied cell migratory and invasive signalling profiles, we utilised MPNST cell lines with differing levels of c-MET expression. In three of the four MPNST cell lines (ST8814, S1844.1 and S1507.2), exhibiting elevated expression of c-MET, cell migration was potently blocked upon inhibition of c-MET. Importantly, we show that Signal Transducer and Activator of Transcription 3 (STAT3), which is positioned downstream of multiple receptor tyrosine kinase signalling inputs including c-MET, functions as a central driver of cell migration and tumour formation in all four MPNST cell lines examined (ST8814, S462, S1844.1 and S1507.2). This work indicates that STAT3 could be a viable pharmacological target for treatment of MPNSTs alongside other pharmacological targets such as receptor tyrosine kinases.

2. Material and methods

2.1. Antibodies

Antibodies against phosphorylated STAT3 at Tyr705 (# 9145), and Ser727 (#9134), total STAT3 (#4904) and total β-actin (13E5, #4970) were purchased from Cell Signalling Technology Inc. (Danvers, MA, U.S.A.). Antibodies against phosphorylated c-MET (Tyr1234/1235; #05-900) and total c-MET (#sc162) was purchased from Millipore U.K. Limited (Watford, U.K.) and Santa Cruz Biotechnology Inc. (Heidelberg, Germany), respectively.

2.2. Cell lines and maintenance

ST8814 MPNST-derived cell lines were purchased from ATCC (distributed by LGC Standards, Middlesex, UK). The S462, S1844.1 and S1507.2 MPNST cell lines were a kind gift from Prof. Mautner, (University of Hamburg, Germany) and the late Prof. Guha, (University of Toronto, Canada), the MDA-MB-231 cell line was provided by Dr. Zaruhi Poghosyam (Cardiff University, Cardiff, U.K.). Cell lines were cultured and maintained in Dulbecco's Modified Eagle Medium (DMEM) supplemented with 10% (v/v) Fetal Bovine Serum (FBS) and 1% (v/v) Penicillin-Streptomycin in a humidified incubator (5% CO2 at 37^{o}C). All cells were routinely screened for mycoplasma and were uncontaminated (MycoAlert Detection Kit from Lonza Biologicals Plc., Slough, U.K.).

2.3. Drug treatments

PF-04217903 was a kind gift from Pfizer Limited. Cells were pre-treated for 30 min prior to HGF stimulation. All experiments were performed in triplicate. Cucurbitacin-I, 5,15-DPP, FLLL31, SU11274, rapamycin and all other reagents unless otherwise stated were purchased from Sigma-Aldrich Company Ltd. (Dorset, U.K.). IL-6, HGF and PDGF (R&D systems Abingdon, U.K.) were used for stimulation.

2.4. Cell Lysis and Immunoprecipitation

Cells were lysed using a pP40 lysis buffer (50 mM Tris-HCl, 0.5 M NaCl, pH 7.4, 50 mM β-glycophosphate, 5 mM $MgCl_2$, 10% (v/v) glycerol and 1% (v/v) Nonidet-P40 supplemented with a Mini complete mini Protease Inhibitor Cocktail (Roche Diagnostics Ltd., Burgess Hill, U.K.). Protein concentrations were assessed with use of Bradford reagent, as instructed from the manufacture in accordance with manufacturer protocol (Sigma-Aldrich Company Ltd. (Dorset, U.K.). c-MET was immunopreciptated using anti-c-MET antibodies coupled to G-Sepharose beads (GE Healthcare Lifesciences, Buckinghamshire, U.K.), and washed three times in lysis buffer and resolved by SDS-PAGE. Samples for STAT3 analysis were prepared by direct lysis in sample buffer (62.5 mM Tris-HCL, 50 mM DTT, 2% (w/v) SDS, 10% (v/v) Glycerol and 0.1% (w/v) Bromophenol blue, pH 7.6) and sonicated (Bioruptor from Diagenode) for 5 x 40 s cycle pulses.

2.5. Western Blot

The NuPage Novex gel system was used for electrophoresis as described in the manufacturers protocol (Life Technology, Paisley, UK). Depending on the protein size, protein samples were resolved on either 3-8% Tris-acetate or 4-12% Bis-Tris gels. Proteins were then transferred to a polyvinylidene fluoride membrane purchased from Millipore U.K. Ltd. (Watford, U.K.), blocked in 5% (w/v) dry milk powder in standard Tris-Buffer Saline supplemented with 0.1% (v/v) Tween (as recommended by Cell Signalling Technology Inc. (Danvers, MA, U.S.A.)) for 4 h. Membranes were incubated at 4 ^{o}C overnight in primary antibody in 2% (w/v) BSA in TBS-T, then washed twice for 4 min in TBS-T and incubated in the appropriate HRP-conjugated secondary antibody (1:10,000 dilution in TBS-T) for a minimum of 30 min at room temperature. Membranes were washed four times for 3 min with TBS-T and then incubated in Enhanced Chemiluminesence solution (GE Healthcare Lifesciences, Buckinghamshire, U.K.) for 1 min. Konica Medical Film was used to visualise the signal and the exposed films were developed using a Konica Minolta SRX-101A developer.

2.6. Analysis of c-MET mRNA in MPNST

TRIzol (Life Technology, Paisley, U.K.) was used as described in the manufactures protocol for mRNA extraction from benign neurofibromas and MPNSTs obtained from patients. This project was approved by the local Ethics committee. Informed consent for sample collection was obtained according to protocols approved by this committee. Cell lines were harvested in RT-protect buffer (Qiagen, West Sussex, U.K.) and centrifuged at 5,000 rpm for 5 min. mRNA was extracted from the pellet using the Qiagen mRNA extraction kit in accordance with manufacturer's protocol. QIA shredders were utilized to homogenize the pellet (Qiagen, West Sussex, U.K.). mRNA concentration and purity was assessed by using a nanodrop spectrophotometer. Total RNA from each sample (1 µg) was transcribed into complementary cDNA using a Quantitect reverse transcription kit (Qiagen, West Sussex, U.K.) in a thermal cycler (Applied Biosystems). The sequences of the c-MET primers used were forward 5'-CCACCACAGTCCCCAGAGT-3' and reverse 5'-AGATCACATGAACACAGGA-3', with an amplicon size of 51 base pairs. β-actin with an amplicon size of 104 base pairs (cat no. QT01680476) was purchased from Qiagen who retain the right to withhold primer sequence information. β-actin was used as a control. Quantitative real-time PCR reactions were conducted in 96-well plates using appropriate primer assays and SYBR Green PCR Master mix (Qiagen, West Sussex, U.K.). Assays were performed as follows: Initial denaturation step (95 °C, 15 min), 40 cycles of denaturation (94 °C, 15 s), annealing step (55 °C, 30 s), extension step (72 °C, 40 s). The amplification products were quantified during the extension step in the fortieth cycle. The results were then determined using the delta-delta-Ct method, and standardized to β-actin control. A dissociation step was performed, which verified that only one PCR product was produced with each primer set and shows their specificity. The correct size of PCR products was also verified by resolution on 1% (v/v) agarose gels.

2.7. Wound healing

Cells were seeded in 60 mm plates and left to reach 100% confluency. Cells were then synchronised in 1% (v/v) FBS DMEM for 24 h and "wounded" with a pipette tip. Dead cells were removed with PBS wash and then subsequently replaced with DMEM (10% (v/v) FBS). Cells were pre-treated for 30 min with either rapamycin, c-MET or STAT3 inhibitors (where indicated) before cytokine stimulation. Pictures were taken before treatment and 12-18 h after treatment using an inverted AMG EVOS microscope equipped with an Olympus camera.

2.8. Migration and Invasion Assays

Transwell permeable supports with 6.5 mm diameter inserts, 8.0 µm pore size and a polycarbonate membrane (Corning, cat no: 3428) were used to perform migration assays. Cells were grown in a 75cm^2 flask with standard medium (10% (v/v) FBS) until confluent. Cells were then harvested using Trypsin-EDTA. Cells were counted using a haemocytometer. 1x10^6 cells were resuspended in DMEM containing 1% (v/v) FBS. These cells were then seeded in the upper chamber of the Transwell; the lower chamber was filled with 600 µl of standard culture medium (10% (v/v) FBS) and 5 mg/ml fibronectin (R&D systemsm, Abingdon, U.K.), as an adhesive substrate. Cells were incubated at 37 ^oC 5% CO_2 for 24 h. The percentage of adherent cells was then determined by fixing the cells with methanol and acetone (1:1) for 20 min at -20°C. Cells were then stained with Crystal Violet (5 mg/ml) in ethanol for 10 min, followed by a stringent wash with dH_2O until the water ran clear. Crystal violet stained cells were eluted with 1% (w/v) SDS and the absorbance was read at 550 nm on a Genova MK3 Lifescience Analyser (Jenway Scientific, Straffordshire, U.K.). For invasion assays, a similar protocol was employed; however the top chamber of the Transwell was filled with 300 µl of BD Matrigel Basement Membrane Matrix (1 mg/ml). The Matrigel was incubated at 37 ºC for 4 h to allow it to gel. Cells were then seeded and incubated as mentioned in migration assay for 3 days. The number of invaded cells was determined by fixation and staining and elution of crystal violet with 1% (w/v) SDS, as before.

2.9. Lentivirus generation and shRNA knockdown of STAT3

Both STAT3 shRNA (Clone ID: NM_003150.3-458s21c1) and non-target control MISSION shRNA (Clone ID: SHCO16) in pLKO.1 vector (Sigma-Aldrich Company Ltd. (Dorset, U.K.)) were packaged into lentivirus using HEK293T cells co-transfected (lipofectamine 2000, Life Technology, Paisley, U.K.) with pLP1, pLP2, and pLP (VSVG). Confluent MPNST cell lines were infected with shRNA containing lentivirus (STAT3 or non-target control) and selected over 2 weeks with 5 µg/ml puromycin (Life Technology, Paisley, U.K.). Puromycin selected mixed cell populations were then used for cell migration and tumour formation assays.

2.10. Tumour spheroid assays

Two-layered soft agar assays were carried out in six-well plates. MPNST cell lines were plated in complete DMEM media in 0.35% (v/v) agar at (3 x 10x^5) over a 0.6% (v/v) agar layer. The agar was then overlaid with complete DMEM media supplemented with 0.1 µM puromycin (Life Technology, Paisley, U.K.), and then colonies of MPNSTs were grown for 14 days at 37 °C in 5% CO2. Media was changed twice a week. Pictures were taken using an

inverted AMG EVOS microscope equipped with an Olympus camera. Volume of tumour spheroids was measured using ImageJ software.

3. Results

3.1. Gene-expression amplification of c-MET in MPNSTs

To analyse c-MET expression in MPNSTs, we compared the levels of c-MET mRNA between benign neurofibromas and MPNST tissue from NF1 patients (Figure 1A). Compared with seven benign controls, eight out of fourteen MPNST tissues had elevated levels of c-MET mRNA. We extended this study to a range of MPNST-derived cell lines (Figure 1B). Similar to the MPNST tissue, we found variance in the levels of c-MET mRNA. In particular, ST8814 cells had 3-fold amplification of c-MET mRNA, when compared to the S462, which had a much lower level of c-MET mRNA. The breast cancer cell line, MDA-MB-231, acts as positive control, with expected high levels of *c-MET* expression.

3.2. c-MET inhibition potently impairs wound healing of ST8814 cells, while S462 cells are unaffected

Given that we observe significant differences in the expression levels of *c-MET* within various MPNST-derived cell lines; we postulated that they may exhibit differential sensitivity to *c-MET* inhibition. We compared the highest *c-MET* expressing MPNST cell line, ST8814, with that of S462 (which had the lowest level of *c-MET* expression of the cell lines analysed). In both these MPNST derived cell lines, the c-MET inhibitors, SU11274 and PF-4217903, were sufficient to block HGF induced c-MET activation, as observed by a reduction in Tyr1234/1235 phosphorylation of c-MET (Figure 2A and 2B). Of interest, platelet-derived growth factor (PDGF) also potently activated c-MET in both the ST8814 (Figure 2A) and S462 cells (Figure 2B), revealing signalling cross talk between the PDGF receptor (PDGF-R) and c-MET. Signalling cross talk from receptor tyrosine kinases to c-MET has also been proposed in urothelial bladder cancer (Lan et al., 2013; Yeh et al., 2011). Previous work indicated that inhibition of c-MET blocked cell migration and invasion of the ST8814 cell line (Su et al., 2004; Torres et al., 2011). We show that HGF induced wound healing in the ST8814 cells was significantly reduced after inhibition of c-MET with both the SU11274 and PF-4217903 inhibitors (Figure 2C). In contrast to the ST8814 cells, HGF induced cell migration of the S462 cell line was completely insensitive to c-MET inhibition during the 12 h wound healing assay (Figure 2D). Considering that cellular doubling time is approximately 24 h for the ST8814 cells and 16 h for the S462 cells (Lopez et al., 2011) (data not shown), cell migration during this 12 h period of wound healing is unlikely to be influenced by differences in cell proliferation. These results suggest that instead of utilising the migratory HGF/c-MET signalling pathway for wound healing, the S462 cell line is more dependent

upon other migratory cell signalling pathways. Similar to the ST8814 cells, wound healing in both the S1507.2 and S1844.1 cell lines were potently inhibited with SU11274 and PF-4217903 drug treatment (Figure 2E). This data reveals that HGF induced cell migration in multiple MPNST cell lines can be highly sensitive to inhibition to c-MET.

3.3. ST8814 and S462 cells have markedly different STAT3 signalling profiles after HGF stimulation

One mechanism by which c-MET drives cell motility is through activation of the JAK2/STAT3 signalling pathway. *STAT3* is considered an oncogene and promotes transcription of genes linked to cancer progression including cell migration, invasion, and survival (Kermorgant and Parker, 2008). In the ST8814 cells, tyrosine phosphorylation of STAT3 was robustly induced after just 30 min of HGF stimulation and was maintained throughout the 3 h time course, which was not evident in either of the S462 or S1507.1 cells (Figure 3). It is probable that amplification of HGF/c-MET signalling in these ST8814 cells is responsible for such a robust and enduring STAT3 signal after HGF stimulation. Conversely, HGF stimulation within the S462 and S1507.2 cell lines resulted in a much slower and less pronounced level of STAT3 activation over the 3 h time course (Figure 3). Cells were also stimulated with interleukin-6 (IL-6) for 30 min as a positive control for STAT3 activation, illustrating that signalling through many receptor tyrosine kinases in MPNSTs can potently activate STAT3. Of interest, IL-6 is also known to be elevated in Schwann cells lacking *NF1* (Kawachi et al., 2013).

3.4. Inhibition of STAT3 impairs wound healing in multiple MPNST cell lines

To examine the involvement of STAT3 in cell migration, we employed three different STAT3 inhibitors; Cucurbitacin-I, 5,15-diphenylporphyrin (5,15-DPP) and FLLL31. Cucurbitacin-I and FLLL31 are derived from curcumin and both selectively bind to and inhibit the tyrosine kinase Janus kinase 2 (JAK2), which is immediately upstream of STAT3. 5,15-DPP is a selective STAT3- Src homology-2 domain (SH2) antagonist, where 5,15-DPP prevents STAT3 SH2 domain-mediated ligand binding, dimerisation and propagation of signal transduction. All three inhibitors suppressed HGF-induced tyrosine phosphorylation of STAT3 in both the ST8814 (Figure 4A) and S462 cell lines (Figure 4B). Ser727 phosphorylation of STAT3 in both ST8814 and S462 cell lines was less sensitive to drug treatments. Ser727 is considered to be phosphorylated directly by mTORC1 (Yokogami et al., 2000). Next we analysed the effects of STAT3 inhibition on cell migration during wound healing in the ST8814 (Figure 4C) and S462 cell lines (Figure 4D) as well as the S1844.1 and S1507.2 cell lines (Figure 4E). 5,15DPP showed no significant effect in inhibiting wound healing in 3 of the MPNST cell lines (ST8814, S462 and S1507.2), while FLLL31 blocked

wound healing in all MPNST cell lines tested. Cucurbitacin-I blocked wound healing in the ST8814 and S462 cells however it greatly altered the morphology of the S1844.1 and S1507.2 cell lines (supplementary Figure S1) causing detachment of these cells. Consequently, wound healing assay data was unattainable using cucurbitacin-I with these S1507.2 and S1844.1 cell lines.

3.5. STAT3 inhibition impairs cell migration and invasion in both ST8814 and S462 cell lines, while c-MET inhibition is more selective for the ST8814 cell line

We next carried out migration and invasion assays in both the ST8814 and S462 cell lines and analysed the effectiveness of c-MET and STAT3 inhibitors in suppressing both cell migration (Figure 5A) and invasion (Figure 5B). In the ST8814 cell line, inhibition of either c-MET or STAT3 significantly decreased cell migration and invasion. Conversely, cell migration and invasion within S462 cells was only significantly suppressed by STAT3 inhibition. The insensitivity of the S462 cells to c-MET inhibitor is likely due to the lower levels of c-MET amplification that we observe in these cells. Both ST8814 and S462 cells were markedly sensitive to STAT3 inhibition, revealing that they too are both dependent upon STAT3 signalling for their migratory and invasive properties.

3.6. Within multiple MPNST cell lines, rapamycin has no additive effect at impairing wound healing when combined with c-MET inhibitors

Given that mTORC1 is considered an upstream kinase of STAT3 via Ser727 phosphorylation (Yokogami et al., 2000), we next examined whether mTORC1 inhibition with rapamycin could further impair wound healing in these MPNST cell lines when combined with c-MET inhibitors. We observed that treatment with rapamycin had very little additive effect on wound healing in any of the MPNST cell lines tested when combined with either SU11274 or PF-4217903 (Figure 6). As a single agent, rapamycin had varied effect on cell migration within these 4 MPNST cell lines. The ST8814 (70% reduction) and S1844.1 (45% reduction) cells were more sensitive, while the S462 and S1507.2 were the least sensitive (with no significant change).

3.7. STAT3 knockdown in multiple MPNST cell lines impair wound healing and tumour formation

Our data highlights that STAT3 is required for optimal cell migration within these 4 MPNST cell lines. To confirm the importance of STAT3, we knocked down gene-expression of STAT3 in these 4 MPNST cell lines (Figure 7) and examined their capacity to heal a wound

(Figure 7, upper graph). In all these MPNST cell lines, knockdown of STAT3 robustly inhibited wound closure by over 50%. Furthermore, STAT3 knockdown impacted the tumour spheroid volume in all MPNST cell lines tested in soft agar (Figure 7, lower graph), which again further strengthens the involvement in STAT3 in promoting tumourgenesis and malignancy in multiple MPNSTs with varied signalling profiles. This rational is supported by earlier studies showing that the STAT3 inhibitors, JSI-124 and FLLL32 delayed tumour formation in a MPNST xenograft nude mouse models using the ST8814 cell line (Banerjee et al., 2010; Wu et al., 2013).

Discussion

Although it is known that somatic *NF1* gene inactivation results in aberrant Ras signalling, it is evident that activation of Ras alone is not sufficient to induce malignant transformation. In this study, we show that both c-MET and STAT3 signalling pathways contribute to malignancy in multiple MPNSTs. We reveal that cell migration within multiple MPNST cell lines is acutely sensitive to both c-MET and STAT3 inhibition. The transcriptional activity of STAT3 is regulated by JAK2-mediated phosphorylation of Tyr705, where JAK2/STAT3 functions downstream of many different receptor tyrosine kinases. In MPNSTs, there appears to be several key receptor tyrosine kinases that activate the JAK2/STAT3 pathway (refer to Figure 8), which includes (but is not limited to) c-MET, PDGF receptors (PDGF-R) and Interleukin receptors (IL-R). Furthermore, it has been shown that *EGF-R* activates JAK2/STAT3 and is necessary for MPNST transformation (Wu et al., 2013). Sensitivity to c-MET inhibitors within the four MPNST cell lines examined in this study (ST8814, S462, S1507.2 and S1844.1) appeared to directly correlate with the levels of *c-MET* expression. For instance, there was a greater reduction of cell migration and invasion upon c-MET inhibition in MPNST cell lines that displayed a higher level of *c-MET* expression. Of interest, we observed that PDGF stimulation of MPNST cells also led to robust activation of c-MET. This finding reveals that MPNST cells have signalling cross-talk between PDGF-R and c-MET. PDGFR-β expression is known to transform Schwann cells lacking *NF1* (Badache and De Vries, 1998), implying that *PDGF-R*β amplification might be involved in Schwann cell hyperplasia. In a more recent study using a panel of 11 MPNST tumours, *PDGF-R*α, *PDGF-R*β and *EGF-R* were shown to be over-expressed when compared to benign controls and correlates with a higher level of PI3K/Akt/mTORC1 signal transduction (Perrone et al., 2009; Wu et al., 2013). It is possible that some of the transforming potential through PDGF-R might be via signalling cross-talk towards c-MET.

Enhanced signalling through interleukin (IL) to STAT3 is also known to be involved in tumourigenesis (for review see (Bowman et al., 2000)), however the connection between NF1 and IL signalling has not been well studied to date. One piece of evidence implicates IL-6 to NF1 tumourigenesis, where IL-6 was observed to be elevated in Schwann cells lacking NF1 (Lasater et al., 2010). Although further studies will be required, it is possible that signalling through IL-R further promotes malignancy in MPNSTs through activation of the JAK2/STAT3 pathway. We propose that STAT3 could be an attractive 'common' target of therapy with regards to treating MPNSTs with heterogeneity in their migratory/invasive signalling profiles. Recently, Upadhyaya *et al.* (2012) used Affymetrix SNP 6.0 Array analysis to identify a role for increased gene expression of members of the Rho-GTPase pathway in malignancy and metastasis in MPNSTs. It is of interest that signal transduction through STAT3 is a critical driver of Rho (Aznar and Lacal, 2001; Aznar et al., 2001; Debidda et al., 2005). It was shown that inhibition of mTORC1 with rapamycin suppressed the growth of tumours in NF1 mouse models (Hegedus et al. 2008). It is apparent that many genetic alterations found in MPNSTs lead to amplification of signal transduction pathways that enhance either JAK2/STAT3 or mTORC1/STAT3 signalling. For instance, Phosphatase and tensin homolog (PTEN) loss is known to occur in both MPNSTs and epithelioid sarcomas (Keng et al., 2012; Xie et al., 2011) that gives rise to aberrant signalling through PI3K/mTORC1 (see Figure 8).

There are currently no universal prognostic or predictive biomarkers for MPNSTs in terms of their accumulated genetic mutations and their phenotypic expression although several recent studies appear to be promising (Beert et al., 2011; Brekke et al., 2010; Chai et al., 2010; Kresse et al., 2008; Largaespada and Ratner, 2013; Luscan et al., 2013; Mantripragada et al., 2009; Miller et al., 2006; Mo et al., 2013; Pemov et al., 2010; Rahrmann et al., 2013; Subramanian et al., 2010; Upadhyaya et al., 2012; Watson et al., 2013). In a recent elegant study, recurrent homozygous loss of the *CDKN2A* locus was identified in 15/16 atypical neurofibromas supporting that atypical neurofibromas are intermediates between benign neurofibroma and MPNST (Beert et al., 2011). This study suggests that *CDKN2A* loss is an early step in the progression of neurofibroma to MPNSTs.

Given that we observe *c-MET* amplification in more than 50% of MPNSTs from NF1 patients (Figure 1A); our work suggests that *c-MET* expression could be a valid predictive marker of malignancy in NF1 patients. Although evaluation of molecular abnormalities in tumours on an individual basis might help design tailor made therapy, there are limitations to this approach with regards to therapy with regards to MPNSTs. As a result of intra-tumoural molecular heterogeneity in MPNSTs, tumour profiling is difficult to ascertain. Instead, it may be more feasible to develop a therapeutic strategy that targets multiple pathways which are

commonly dysregulated in MPNSTs. With notion in mind, it may be a more feasible to inhibit multiple receptor tyrosine kinases that converge on JAK2/STAT3 as a broader therapeutic strategy to treat NF1 patients. For instance, receptor tyrosine kinase inhibitors are commonly used as therapeutic agents for various malignancies (Engelman and Settleman, 2008).

In summary, our work indicates that cell signalling through both c-MET and STAT3 are common underlying molecular mechanisms involved in MPNST tumourigenesis. Given the dependency of c-MET and STAT3 for cell migration in multiple MPNSTs, therapeutic strategies that target these pathways could be a viable option for NF1 patients.

Conflict of interest statement

The authors have no conflicts of interest to declare.

Acknowledgements

We thank Pamela Bramble from Pfizer for providing the c-MET inhibitor, PF-4217903. We also thank Professors Mautner and Guha for MPNST cell lines. This work was funded by the Association for International Cancer Research (Career Development Fellowship [No.06-914/915] (to A.R.T.)) and the Ian Owen Trust (to M.U.). E.M.R's Ph.D. studentship is funded through the Cancer Genetics Biomedical Research Unit (CGBRU), which is supported by the National Institute of Health and Social Care Research (NISCHR) from the Welsh government. Further support was provided via Wales Gene Park through NISCHR.

Figure Legends

Figure 1 – Gene-expression of *c-MET* is frequently elevated in MPNSTs. c-MET mRNA levels, standardised to β-Actin, was assessed in A) benign versus malignant tumours from NF1 patients as well as B) four NF1-MPNST cell lines (ST8814, S462, S1844.1 and S1507.2), compared to a positive breast cancer cell line with enhanced levels of c-MET mRNA, MDA-MB-231. n = 3. * $p < 0.05$ when comparing either benign versus malignant tumours in A), or MPNST cell lines to S462 in B).

Figure 2 – c-MET inhibition potently impairs HGF induced wound healing of ST8814 cells, while S462 cells are resistant to c-MET inhibition. A-B) Where indicated, starved ST8814 and S462 cells were pre-treated with 10 nM SU11274 and 7.5 ng/µl PF-4217903 for 30 min prior to 30 min stimulation (10 ng/ml PDGF, 20 ng/ml IL-6, and 20 ng/ml HGF). DMSO

vehicle only was used as a control. Total and phosphorylated c-MET (Try1234/1235) was analysed. C) ST8814, D) S462, E) S1507.2 and S1844.1 cells were subjected to wound healing assays after 20 ng/ml HGF stimulation for 12 h in the presence or absence of 10 nM SU11274 and 7.5 ng/µl PF-4217903. n = 3. * $p < 0.05$ when comparing wound closure of treated versus untreated cells.

Figure 3 – ST8814 and S462 cells have markedly different STAT3 signalling profiles after HGF stimulation. A) Starved ST8814, S462 and S1507.2 cells were stimulated with 20 ng/ml HGF for the indicated time (0 h, 1 h, 2 h, and 3 h). Total and phosphorylated STAT3 (Tyr 705) was determined from protein lysates.

Figure 4 – STAT3 inhibition potently impairs wound healing in multiple MPNST cell lines. A) Where indicated, starved A) ST8814 and B) S462 cells were pre-treated with 5 nM Cucurbitacin-I, 50 nM 5,15-DPP and 5nM FLLL31 for 30 min prior to 30 min 20 ng/ml HGF stimulation. DMSO vehicle only was used as a control. From protein lysates, total and phosphorylated STAT3 (Tyr 705 and Ser727), as well as p-rpS6 and β-actin were analysed. C) ST8814 and D) S462, were subjected to wound healing assays after 20 ng/ml HGF stimulation for 12 h in the presence or absence of 5 nM Cucurbitacin-I, 50 nM 5,15-DPP and 5 nM FLLL31. E) S1844.1 and S1507.2 cells were subjected to wound healing assays after treatment with 50 nM 5,15-DPP and 5 nM FLLL31. Wound healing (%) of the MPNSTs after drug treatment compared to untreated is shown as a graph. n = 3. * $p < 0.05$ when comparing wound closure of treated versus untreated cells.

Figure 5 – Cell migration and invasion in ST8814 and S462 cells are both highly sensitive to STAT3 inhibition. A) Cell migration and B) cell invasion assays were carried out on ST8814 and S462 cells in the presence or absence of 10 nM SU11274 and 5 nM FLLL31 prior to 20 ng/ml HGF stimulation , where indicated. DMSO vehicle only was used as a control. n = 3. * $p < 0.05$ when comparing treated versus untreated cells.

Figure 6 – Rapamycin inhibits wound healing in the ST8814 and S1844.1 cells while S462 and S1507.2 cells are less sensitive. ST8814, S462, and S1844.1 and S1507.2 cells were subjected to wound healing assays after 20 ng/ml HGF stimulation for 12 h in the presence or absence of 10 nM SU11274, 7.5 ng/µl PF-4217903 and 50 nM Rapamycin, where indicated. DMSO vehicle only was used as a control. n = 3. * $p < 0.05$ when comparing wound closure of treated versus untreated cells.

Figure 7 – STAT3 knockdown impairs wound healing and tumour formation in soft agar. Stable ST8814, S462, S1844.1 and S1507.2 cell lines, expressing either non-target or

STAT3 shRNA, as indicated, were subjected to either cell wound (upper graph) or tumour spheroid growth assays (lower graph, n=40/ scale bar represents 250 μm). Confirming efficient knockdown, STAT3 protein levels were compared between cell lines by western blot, and β-actin serves as a loading control. n = 3. * $p < 0.05$ when comparing treated versus untreated cells.

Figure 8 – PDGF-R, c-MET, and IL-R signalling converge on STAT3 in MPNST cell lines to drive cell metastasis. Inhibitors used in this study include: c-MET inhibitors (SU11274 and PF-4217903), STAT3 inhibitors (Cucurbitacin-I, 5,15-DPP and FLLL31) and mTORC1 inhibitor (Rapamycin). In MPNST cells, there is signalling cross-talk from PDGF-R to c-MET. As well as through c-MET activation, IL-R activation leads to signal transduction through JAK2/STAT3 (Tyr705 phosphorylation of STAT3). Activation of mTORC1 leads to Ser727 phosphorylation of STAT3, which is basally high in MPNSTs.

Supplementary Figure Legends

Supplementary Figure 1 – STAT3 inhibitor, Cururbitacin-1, alters cells morphology of S1844.1 and S1507.2 MPNST cell lines. Both S1844.1 and S1507.2 cell lines were treated with 5 nM Cucurbitacin-I over-night prior to 20 ng/ml HGF stimulation. Bright field images of cell lines are shown, which reveals rounding up of both MPNST cell lines with Cucurbitacin-I treatment.

References

Albritton, K.H., Rankin, C., Coffin, C.M., Ratner, N., Budd, G.T., Schuetze, S.M., Randall, R.L., Declue, J.E., Borden, E.C., 2006 . Phase II study of erlotinib in metastatic or unresectable malignant peripheral nerve sheath tumors (MPNST). ASCO J. Clin. Oncol. 24, 18s (suppl; abstr 9518).

Arun, D., Gutmann, D.H., 2004. Recent advances in neurofibromatosis type 1. Curr. Opin. Neurol. 17, 101–105.

Aznar, S., Lacal, J.C., 2001. Rho signals to cell growth and apoptosis. Cancer Lett. 165, 1–10.

Aznar, S., Valerón, P.F., del Rincon, S. V, Pérez, L.F., Perona, R., Lacal, J.C., 2001. Simultaneous tyrosine and serine phosphorylation of STAT3 transcription factor is involved in Rho A GTPase oncogenic transformation. Mol. Biol. Cell. 12, 3282–3294.

Badache, a, De Vries, G.H., 1998. Neurofibrosarcoma-derived Schwann cells overexpress platelet-derived growth factor (PDGF) receptors and are induced to proliferate by PDGF BB. J. Cell. Physiol. 177, 334–342.

Banerjee, S., Byrd, J.N., Gianino, S.M., Harpstrite, S.E., Rodriguez, F.J., Tuskan, R.G., Reilly, K.M., Piwnica-Worms, D.R., Gutmann, D.H., 2010. The neurofibromatosis type 1 tumor suppressor controls cell growth by regulating signal transducer and activator of transcription-3 activity in vitro and in vivo. Cancer Res. 70, 1356–1366.

Beert, E., Brems, H., Daniëls, B., De Wever, I., Van Calenbergh, F., Schoenaers, J., Debiec-Rychter, M., Gevaert, O., De Raedt, T., Van Den Bruel, A., de Ravel, T., Cichowski, K., Kluwe, L., Mautner, V., Sciot, R., Legius, E., 2011. Atypical neurofibromas in neurofibromatosis type 1 are premalignant tumors. Genes Chromosomes Cancer . 50, 1021–1032.

Bennett, E., Thomas, N., Upadhyaya, M., 2009. Neurofibromatosis type 1 : Its association with the Ras / MAPK pathway syndromes. 7, 105–115.

Birchmeier, C., Birchmeier, W., Gherardi, E., Vande Woude, G.F., 2003. Met, metastasis, motility and more. Nat. Rev. Mol. Cell Biol. 4, 915–925.

Bottaro, D.P., Rubin, J.S., Faletto, D.L., Chan, A.M., Kmiecik, T.E., Vande Woude, G.F., Aaronson, S.A., 1991. Identification of the hepatocyte growth factor receptor as the c-met proto-oncogene product. Science. 251, 802–804.

Bowman, T., Garcia, R., Turkson, J., Jove, R., 2000. STATs in oncogenesis. Oncogene. 19, 2474–2488.

Brekke, H.R., Kolberg, M., Skotheim, R.I., Hall, K.S., Bjerkehagen, B., Risberg, B., Domanski, H. a, Mandahl, N., Liestøl, K., Smeland, S., Danielsen, H.E., Mertens, F., Lothe, R.A., 2009. Identification of p53 as a strong predictor of survival for patients with malignant peripheral nerve sheath tumors. Neuro. Oncol. 11, 514–28.

Brekke, H.R., Ribeiro, F.R., Kolberg, M., Agesen, T.H., Lind, G.E., Eknaes, M., Hall, K.S., Bjerkehagen, B., van den Berg, E., Teixeira, M.R., Mandahl, N., Smeland, S., Mertens, F., Skotheim, R.I., Lothe, R.A., 2010. Genomic changes in chromosomes 10, 16, and X in malignant peripheral nerve sheath tumors identify a high-risk patient group. J. Clin. Oncol. 28, 1573–1582.

Bridge, R.S., Bridge, J. a, Neff, J.R., Naumann, S., Althof, P., Bruch, L.A., 2004. Recurrent chromosomal imbalances and structurally abnormal breakpoints within complex karyotypes of malignant peripheral nerve sheath tumour and malignant triton tumour: a cytogenetic and molecular cytogenetic study. J. Clin. Pathol. 57, 1172–1178.

Chai, G., Liu, N., Ma, J., Li, H., Oblinger, J.L., Prahalad, A.K., Gong, M., Chang, L., Wallace, M., Muir, D., Guha, A., Phipps, R.J., Hock, J.M., 2010. MicroRNA-10b regulates tumorigenesis in neurofibromatosis type 1. Cancer Sci. 101, 1994-2004.

Chugh, R., Wathen, J.K., Maki, R.G., Benjamin, R.S., Patel, S.R., Meyers, P.A., Myers, P.A., Priebat, D.A., Reinke, D.K., Thomas, D.G., Keohan, M.L., Samuels, B.L., Baker, L.H., 2009. Phase II multicenter trial of imatinib in 10 histologic subtypes of sarcoma using a bayesian hierarchical statistical model. J. Clin. Oncol. 27, 3148–3153.

De Raedt, T., Brems, H., Wolkenstein, P., Vidaud, D., Pilotti, S., Perrone, F., Mautner, V., Frahm, S., Sciot, R., Legius, E., 2003. Elevated risk for MPNST in NF1 microdeletion patients. Am. J. Hum. Genet. 72, 1288–1292.

Debidda, M., Wang, L., Zang, H., Poli, V., Zheng, Y., 2005. A role of STAT3 in Rho GTPase-regulated cell migration and proliferation. J. Biol. Chem. 280, 17275–17285.

Ducatman, B.S., Scheithauer, B.W., Piepgras, D.G., Reiman, H.M., Ilstrup, D.M., 1986. Malignant peripheral nerve sheath tumors. A clinicopathologic study of 120 cases. Cancer. 57, 2006–2021.

Ellison, D.A., Corredor-Buchmann, J., Parham, D.M., Jackson, R.J., 2005. Malignant triton tumor presenting as a rectal mass in an 11-month-old. Pediatr. Dev. Pathol. 8, 235–239.

Engelman, J.A., Settleman, J., 2008. Acquired resistance to tyrosine kinase inhibitors during cancer therapy. Curr. Opin. Genet. Dev. 18, 73–79.

Ferner, R.E., Huson, S.M., Thomas, N., Moss, C., Willshaw, H., Evans, D.G., Upadhyaya, M., Towers, R., Gleeson, M., Steiger, C., Kirby, A., 2007. Guidelines for the diagnosis and management of individuals with neurofibromatosis 1. J. Med. Genet. 44, 81–88.

Hegedus, B., Banerjee, D., Yeh, T.H., Rothermich, S., Perry, A., Rubin, J.B., Garbow, J.R., Gutmann, D.H., 2008. Preclinical cancer therapy in a mouse model of neurofibromatosis-1 optic glioma. Cancer Res. 68, 1520–1528.

Holtkamp, N., Reuss, D.E., Atallah, I., Kuban, R.J., Hartmann, C., Mautner, V.F., Frahm, S., Friedrich, R.E., Algermissen, B., Pham, V.A., Prietz, S., Rosenbaum, T., Estevez-Schwarz, L., von Deimling, A., 2004. Subclassification of nerve sheath tumors by gene expression profiling. Brain Pathol. 14, 258–264.

Katz, D., Lazar, A., Lev, D., 2009. Malignant peripheral nerve sheath tumour (MPNST): the clinical implications of cellular signalling pathways. Expert Rev. Mol. Med. 11, e30.

Kawachi, Y., Maruyama, H., Ishitsuka, Y., Fujisawa, Y., Furuta, J., Nakamura, Y., Ichikawa, E., Furumura, M., Otsuka, F., 2013. NF1 gene silencing induces upregulation of vascular endothelial growth factor expression in both Schwann and non-Schwann cells. Exp. Dermatol. 22, 262–265.

Keng, V.W., Watson, A.L., Rahrmann, E.P., Li, H., Tschida, B.R., Moriarity, B.S., Choi, K., Rizvi, T.A., Collins, M.H., Wallace, M.R., Ratner, N., Largaespada, D.A., 2012. Conditional Inactivation of Pten with EGFR Overexpression in Schwann Cells Models Sporadic MPNST. Sarcoma. vol. 2012, Article ID 620834, DOI: 10.1155/2012/620834.

Kermorgant, S., Parker, P.J., 2008. Receptor trafficking controls weak signal delivery: a strategy used by c-Met for STAT3 nuclear accumulation. J. Cell Biol. 182, 855–863.

King, A.A., Debaun, M.R., Riccardi, V.M., Gutmann, D.H., 2000. Malignant peripheral nerve sheath tumors in neurofibromatosis 1. Am. J. Med. Genet. 93, 388–392.

Klose,A., Ahmadian, M.R., Schuelke, M., Scheffzek, K., Hoffmeyer, S., Gewies, a, Schmitz, F., Kaufmann, D., Peters, H., Wittinghofer, A., Nürnberg, P., 1998. Selective disactivation of neurofibromin GAP activity in neurofibromatosis type 1. Hum. Mol. Genet. 7, 1261–1268.

Korf, B., Widemann, B., Acosta, M.T., Packer, R.J., 2012. Translational/Clinical Studies in Children and Adults with Neurofibromatosis Type 1, in: Upadhyaya, M., Cooper, D. (Eds.), Neurofibromatosis Type 1. Springer-Verlag., Berlin Heidelberg, pp.625-657.

Krasnoselsky, A., Massay, M.J., DeFrances, M.C., Michalopoulos, G., Zarnegar, R., Ratner, N., 1994. Hepatocyte growth factor is a mitogen for Schwann cells and is present in neurofibromas. J. Neurosci. 14, 7284–7290.

Kresse, S.H., Skårn, M., Ohnstad, H.O., Namløs, H.M., Bjerkehagen, B., Myklebost, O., Meza-Zepeda, L.A., 2008. DNA copy number changes in high-grade malignant peripheral nerve sheath tumors by array CGH. Mol. Cancer 7, 48-59.

Lan, S., Wu, S., Raghavaraju, G., 2013. The Crosstalk of c-MET with Related Receptor Tyrosine Kinases in Urothelial Bladder Cancer, in: Persad, R., Weranja, R. (Eds.), Advances in the Scientific Evaluation of Bladder Cancer and Molecular Basis for Diagnosis and Treatment. InTech., National Cheng Kung University , pp. 21-39.

Largaespada, D., Ratner, N., 2013. Interweaving the strands: β-catenin, an HIV co-receptor, and Schwann cell tumors. Cancer Cell. 23, 269–271.

Lasater, E.A., Li, F., Bessler, W.K., Estes, M.L., Vemula, S., Hingtgen, C.M., Dinauer, M.C., Kapur, R., Conway, S.J., Jr, D.A.I., 2010. Genetic and cellular evidence of vascular inflammation in neurofibromin-deficient mice and humans. JCI. 120, 859-870.

Lopez, G., Torres, K., Liu, J., Hernandez, B., Young, E., Belousov, R., Bolshakov, S., Lazar, A.J., Slopis, J.M., McCutcheon, I.E., McConkey, D., Lev, D., 2011. Autophagic survival in resistance to histone deacetylase inhibitors: novel strategies to treat malignant peripheral nerve sheath tumors. Cancer Res. 71, 185–196.

Lothe, R.A., Karhu, R., Mandahl, N., Mandahi, N., 1996. Gain of 17q24-qter detected by comparative genomic hybridization in malignant tumors from patients with von Recklinghausen's neurofibromatosis.Cancer Res. 56, 4778–4781.

Luscan, A., Shackleford, G., Masliah-Planchon, J., Laurendeau, I., Ortonne, N., Varin, J., Lallemand, F., Leroy, K., Dumaine, V., Hivelin, M., Borderie, D., De Raedt, T., Valeyrie-Allanore, L., Larousserie, F., Terris, B., Lantieri, L., Vidaud, M., Vidaud, D., Wolkenstein, P., Parfait, B., Bieche, I., Massaad, C., Pasmant, E., 2013. The activation of the WNT signalling pathway is a hallmark in Neurofibromatosis type 1 tumorigenesis. Clin. Cancer Res. Advance online publication. DOI: 10.1158/1078-0432.CCR-13-0780.

Maki, R.G., D'Adamo, D.R., Keohan, M.L., Saulle, M., Schuetze, S.M., Undevia, S.D., Livingston, M.B., Cooney, M.M., Hensley, M.L., Mita, M.M., Takimoto, C.H., Kraft, A.S., Elias, A.D., Brockstein, B., Blachère, N.E., Edgar, M. a, Schwartz, L.H., Qin, L.-X., Antonescu, C.R., Schwartz, G.K., 2009. Phase II study of sorafenib in patients with metastatic or recurrent sarcomas. J. Clin. Oncol. 27, 3133–3140.

Mantripragada, K.K., Díaz de Ståhl, T., Patridge, C., Menzel, U., Andersson, R., Chuzhanova, N., Kluwe, L., Guha, A., Mautner, V., Dumanski, J.P., Upadhyaya, M., 2009. Genome-wide high-resolution analysis of DNA copy number alterations in NF1-associated malignant peripheral nerve sheath tumors using 32K BAC array. Genes. Chromosomes Cancer. 48, 897–907.

Mantripragada, K.K., Spurlock, G., Kluwe, L., Chuzhanova, N., Ferner, R.E., Frayling, I.M., Dumanski, J.P., Guha, A., Mautner, V., Upadhyaya, M., 2008. High-resolution DNA copy number profiling of malignant peripheral nerve sheath tumors using targeted microarray-based comparative genomic hybridization. Clin. Cancer Res. 14, 1015–1024.

Mautner, V., Asuagbor, F.A., Dombi, E., Fünsterer, C., Kluwe, L., Wenzel, R., Widemann, B.C., Friedman, J.M., Genetics, M., Columbia, B., Canada, J.M.F., 2008. Assessment of benign tumor burden by whole-body MRI in patients with neurofibromatosis 1. Neuro Oncol. 10, 593-598.

Mawrin, C., Kirches, E., Boltze, C., Dietzmann, K., Roessner, A., Schneider-Stock, R., 2002. Immunohistochemical and molecular analysis of p53, RB, and PTEN in malignant peripheral nerve sheath tumors. Virchows Arch. 440, 610–615.

Meadows, A.T., Silber, J., 1985. Delayed Consequences of Therapy For Childhood Cancer. CA. Cancer J. Clin. 35, 271–286.

Miller, S.J., Rangwala, F., Williams, J., Ackerman, P., Kong, S., Jegga, A.G., Kaiser, S., Aronow, B.J., Frahm, S., Kluwe, L., Mautner, V., Upadhyaya, M., Muir, D., Wallace, M., Hagen, J., Quelle, D.E., Watson, M. a, Perry, A., Gutmann, D.H., Ratner, N., 2006. Large-scale molecular comparison of human schwann cells to malignant peripheral nerve sheath tumor cell lines and tissues. Cancer Res. 66, 2584–2591.

Mo, W., Chen, J., Patel, A., Zhang, L., Chau, V., Li, Y., Cho, W., Lim, K., Xu, J., Lazar, A.J., Creighton, C.J., Bolshakov, S., McKay, R.M., Lev, D., Le, L.Q., Parada, L.F., 2013. CXCR4/CXCL12 mediate autocrine cell- cycle progression in NF1-associated malignant peripheral nerve sheath tumors. Cell. 152, 1077–1090.

Naldini, L., Weidner, K.M., Vigna, E., Gaudino, G., Bardelli, A., Ponzetto, C., Narsimhan, R.P., Hartmann, G., Zarnegar, R., Michalopoulos, G.K., Birchmeierl, W., Comoglio, P.M., 1991. Scatter factor and hepatocyte growth factor are indistinguishable ligands for the MET receptor. EMBO. 10, 2867–2878.

Nielsen, G.P., Stemmer-Rachamimov, A.O., Ino, Y., Moller, M.B., Rosenberg, A.E., Louis, D.N., 1999. Malignant transformation of neurofibromas in neurofibromatosis 1 is associated with CDKN2A/p16 inactivation. Am. J. Pathol. 155, 1879–1884.

Pemov, A., Park, C., Reilly, K.M., Stewart, D.R., 2010. Evidence of perturbations of cell cycle and DNA repair pathways as a consequence of human and murine NF1-haploinsufficiency. BMC Genomics 11, 194-210.

Perrone, F., Da Riva, L., Orsenigo, M., Losa, M., Jocollè, G., Millefanti, C., Pastore, E., Gronchi, A., Pierotti, M.A., Pilotti, S., 2009. PDGFRA, PDGFRB, EGFR, and downstream signaling activation in malignant peripheral nerve sheath tumor. Neuro. Oncol. 11, 725–736.

Porter, D.E., Prasad, V., Foster, L., Dall, G.F., Birch, R., Grimer, R.J., 2009. Survival in Malignant Peripheral Nerve Sheath Tumours: A Comparison between Sporadic and

Neurofibromatosis Type 1-Associated Tumours. Sarcoma. vol. 2009, Article ID 756395, doi:10.1155/2009/756395

Rahrmann, E.P., Watson, A.L., Keng, V.W., Choi, K., Moriarity, B.S., Beckmann, D.A, Wolf, N.K., Sarver, A., Collins, M.H., Moertel, C.L., Wallace, M.R., Gel, B., Serra, E., Ratner, N., Largaespada, D.A., 2013. Forward genetic screen for malignant peripheral nerve sheath tumor formation identifies new genes and pathways driving tumorigenesis. Nat. Genet. 45, 756–766.

Scheffzek, K., Ahmadian, M.R., Wittinghofer, A., 1998. GTPase-activating proteins: helping hands to complement an active site. Trends Biochem. Sci. 23, 257–262.

Schuetze, S., Wathen, K., Choy, E., Samuels, B.L., Ganjoo, K.N., Staddon, A.P., von Mehren, M., Chow, W.A., Trent, J.C., Baker, L.H., 2010. Results of a Sarcoma Alliance for Research through Collaboration (SARC) phase II trial of dasatinib in previously treated, high-grade, advanced sarcoma. ASCO J. Clin. Oncol. 28, 15s (suppl; abstr 10009).

Shen, M.H., Mantripragada, K., Dumanski, J.P., Frayling, I., Upadhyaya, M., 2007. Detection of copy number changes at the NF1 locus with improved high-resolution array CGH. Clin. Genet. 72, 238–244.

Storlazzi, C.T., Brekke, H.R., Mandahl, N., Brosjö, O., Smeland, S., Lothe, R.A , Mertens, F., 2006. Identification of a novel amplicon at distal 17q containing the BIRC5/SURVIVIN gene in malignant peripheral nerve sheath tumours. J. Pathol. 209, 492–500.

Su, W., Gutmann, D.H., Perry, A., Abounader, R., Laterra, J., Sherman, L.S., 2004. CD44-independent hepatocyte growth factor/c-Met autocrine loop promotes malignant peripheral nerve sheath tumor cell invasion in vitro. Glia. 45, 297–306.

Subramanian, S., Thayanithy, V., West, R.B., Lee, C., Beck, A.H., Zhu, S., Downs-kelly, E., Montgomery, K., Goldblum, J.R., Hogendoorn, P.C.W., Corless, C.L., Oliveira, A.M., Dry, S.M., Nielsen, T.O., Rubin, B.P., Fletcher, J.A., Fletcher, C.D.M., Rijn, M. Van De., 2010. Genome-wide transcriptome analyses reveal p53 inactivation mediated loss of miR-34a expression in malignant peripheral nerve sheath tumours. J Pathol. 220, 58–70.

Thomas, L., Mautner, V.F., Cooper, D.N., Upadhyaya, M., 2012. Molecular heterogeneity in malignant peripheral nerve sheath tumors associated with neurofibromatosis type 1. Hum. Genomics. 6, 18-27.

Torres, K.E., Zhu, Q.S., Bill, K., Lopez, G., Ghadimi, M.P., Xie, X., Young, E.D., Liu, Juehui, Nguyen, T., Bolshakov, S., Belousov, R., Wang, S., Lahat, G., Liu, Jun, Hernandez, B., Lazar, A.J., Lev, D., 2011. Activated MET is a molecular prognosticator and potential therapeutic target for malignant peripheral nerve sheath tumors. Clin. Cancer Res. 17, 3943–3955.

Tucker, T., Wolkenstein, P., Revuz, J., Zeller, J., Friedman, J.M., 2005. Association between benign and malignant peripheral nerve sheath tumors in NF1. Neurology. 65, 205–211.

Upadhyaya, M., 2010. Neurofibromatosis type 1: diagnosis and recent advances. Expert Opin. Med. Diagn. 4, 307–322.

Upadhyaya, M., 2011. Genetic basis of tumorigenesis in NF1 malignant peripheral nerve sheath tumors. Front. Biosci. 16, 937–951.

Upadhyaya, M., Spurlock, G., Majounie, E., Griffiths, S., Forrester, N., Baser, M., Huson, S.M., Gareth Evans, D., Ferner, R., 2006. The heterogeneous nature of germline mutations in NF1 patients with malignant peripheral serve sheath tumours (MPNSTs). Hum. Mutat. 27, 716–723.

Upadhyaya, M., Spurlock, G., Thomas, L., Thomas, N.S.T., Richards, M., Mautner, V.-F., Cooper, D.N., Guha, A., Yan, J., 2012. Microarray-based copy number analysis of neurofibromatosis type-1 (NF1)-associated malignant peripheral nerve sheath tumors reveals a role for Rho-GTPase pathway genes in NF1 tumorigenesis. Hum. Mutat. 33, 763–776.

Walker, L., Thompson, D., Easton, D., Ponder, B., Ponder, M., Frayling, I., Baralle, D., 2006. A prospective study of neurofibromatosis type 1 cancer incidence in the UK. Br. J. Cancer. 95, 233–238.

Watson, A.L., Rahrmann, E.P., Moriarity, B.S., Choi, K., Conboy, C.B., Greeley, A.D., Halfond, A.L., Anderson, L.K., Wahl, B.R., Keng, V.W., Rizzardi, A.E., Forster, C.L., Collins, M.H., Sarver, A.L., Wallace, M.R., Schmechel, S.C., Ratner, N., Largaespada, D.A., 2013. Canonical Wnt/β-catenin signaling drives human schwann cell transformation, progression, and tumor maintenance. Cancer Discov. 3, 674–689.

Watson, M.A, Perry, A., Tihan, T., Prayson, R. a, Guha, A., Bridge, J., Ferner, R., Gutmann, D.H., 2004. Gene expression profiling reveals unique molecular subtypes of Neurofibromatosis Type I-associated and sporadic malignant peripheral nerve sheath tumors. Brain Pathol. 14, 297–303.

Wu, J., Patmore, D.M., Jousma, E., Eaves, D.W., Breving, K., Patel, A.V, Schwartz, E.B., Fuchs, J.R., Cripe, T.P., Stemmer-Rachamimov, A.O., Ratner, N., 2013. EGFR-STAT3 signaling promotes formation of malignant peripheral nerve sheath tumors. Oncogene. Advance online publication. DOI: 10.1038/onc.2012.579.

Xie, X., Ghadimi, M.P.H., Young, E.D., Belousov, R., Zhu, Q.-S., Liu, J., Lopez, G., Colombo, C., Peng, T., Reynoso, D., Hornick, J.L., Lazar, A.J., Lev, D., 2011. Combining EGFR and mTOR blockade for the treatment of epithelioid sarcoma. Clin. Cancer Res. 17, 5901–5912.

Yeh, C.Y., Shin, S.M., Yeh, H.H., Wu, T.J., Shin, J.W., Chang, T.Y., Raghavaraju, G., Lee, C.T., Chiang, J.H., Tseng, V.S., Lee, Y.C.G., Shen, C.H., Chow, N.H., Liu, H.S., 2011. Transcriptional activation of the Axl and PDGFR-α by c-Met through a ras- and Src-independent mechanism in human bladder cancer. BMC Cancer. 11, 139-151.

Yokogami, K., Wakisaka, S., Avruch, J., Reeves, S.A., 2000. Serine phosphorylation and maximal activation of STAT3 during CNTF signaling is mediated by the rapamycin target mTOR. Curr. Biol. 10, 47–50.

Figure 1

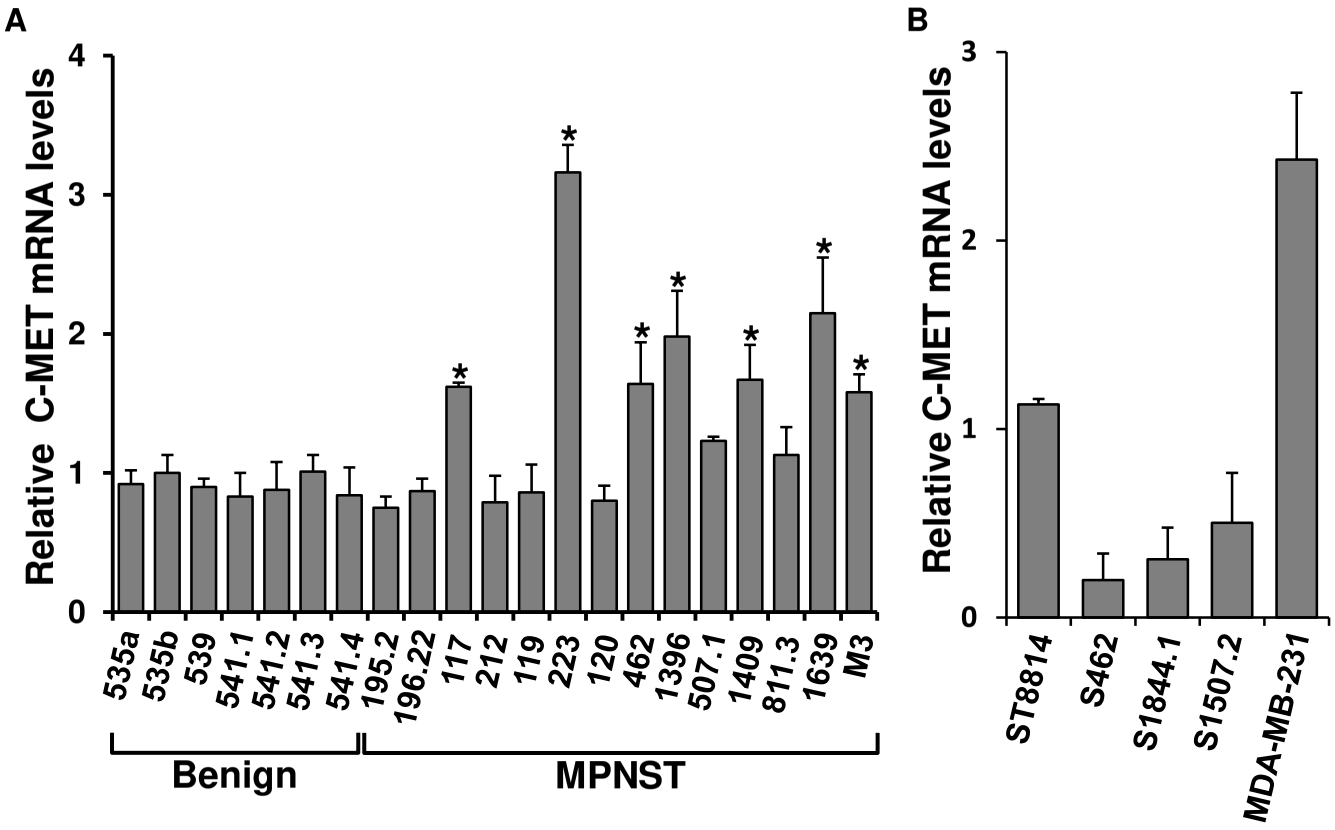
A
Relative C-MET mRNA levels
0
1
2
3
4
535a
535b
539
541.1
541.2
541.3
541.4
195.2
196.22
117
212
119
223
120
462
1396
507.1
1409
811.3
1639
M3
Benign
MPNST
B
Relative C-MET mRNA levels
0
1
2
3
ST8814
S462
S1844.1
S1507.2
MDA-MB-231

Figure 2

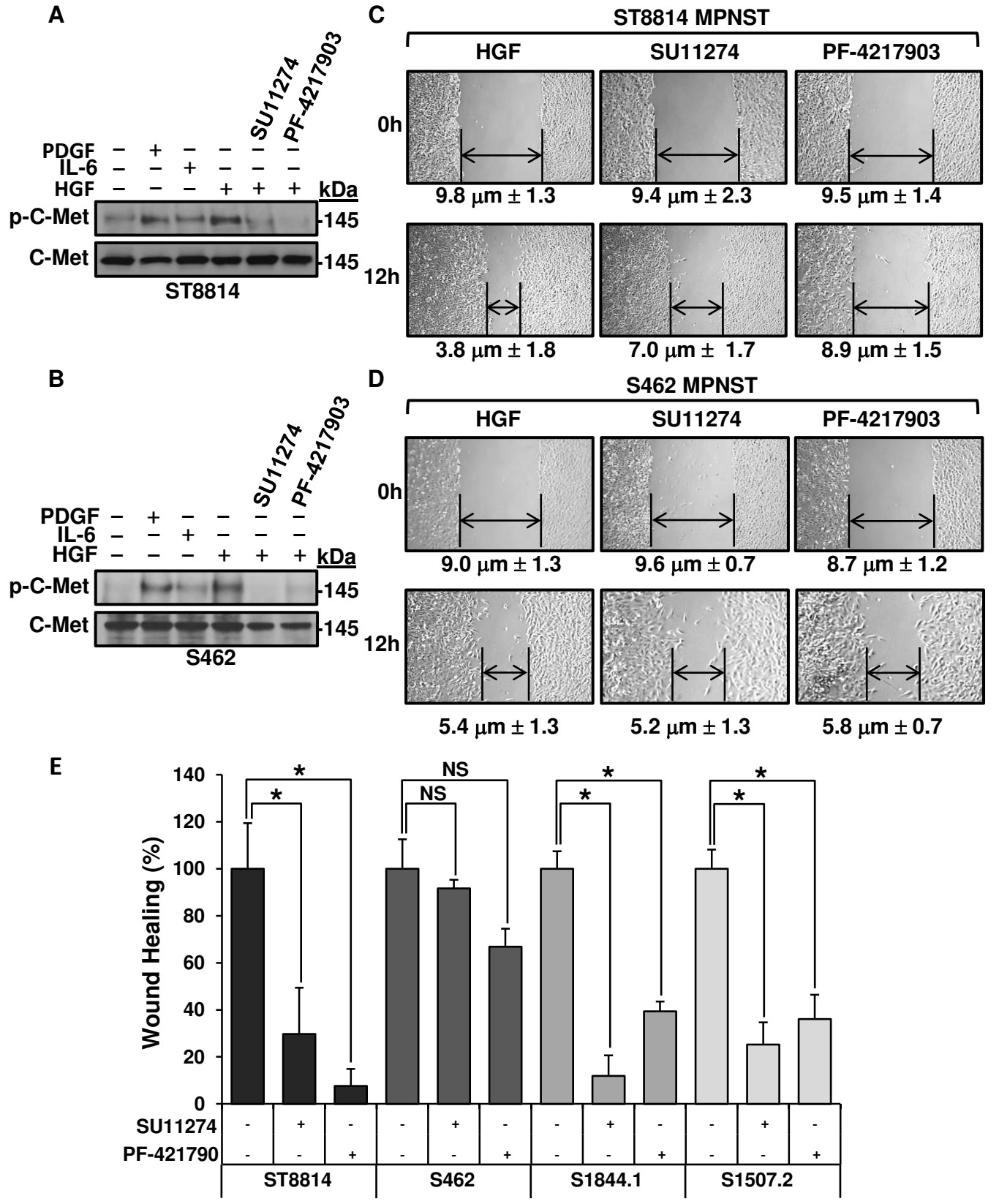
A
SU11274
PF-4217903
PDGF
IL-6
HGF
kDa
p-C-Met
C-Met
145
145
ST8814
B
SU11274
PF-4217903
PDGF
IL-6
HGF
kDa
p-C-Met
C-Met
145
145
S462
C
ST8814 MPNST
HGF
SU11274
PF-4217903
0h
9.8 μm ± 1.3
9.4 μm ± 2.3
9.5 μm ± 1.4
12h
3.8 μm ± 1.8
7.0 μm ± 1.7
8.9 μm ± 1.5
D
S462 MPNST
HGF
SU11274
PF-4217903
0h
9.0 μm ± 1.3
9.6 μm ± 0.7
8.7 μm ± 1.2
12h
5.4 μm ± 1.3
5.2 μm ± 1.3
5.8 μm ± 0.7
E
Wound Healing (%)
140
120
100
80
60
40
20
0
*
*
NS
NS
*
*
*
*
SU11274
PF-421790
ST8814
S462
S1844.1
S1507.2

Figure 3

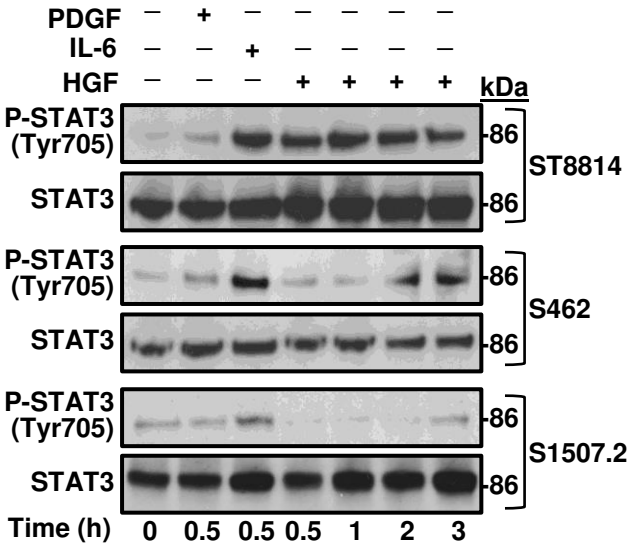
PDGF
IL-6
HGF
kDa
P-STAT3 (Tyr705)
STAT3
86
ST8814
S462
S1507.2
Time (h)
0 0.5 0.5 0.5 1 2 3

Figure 4

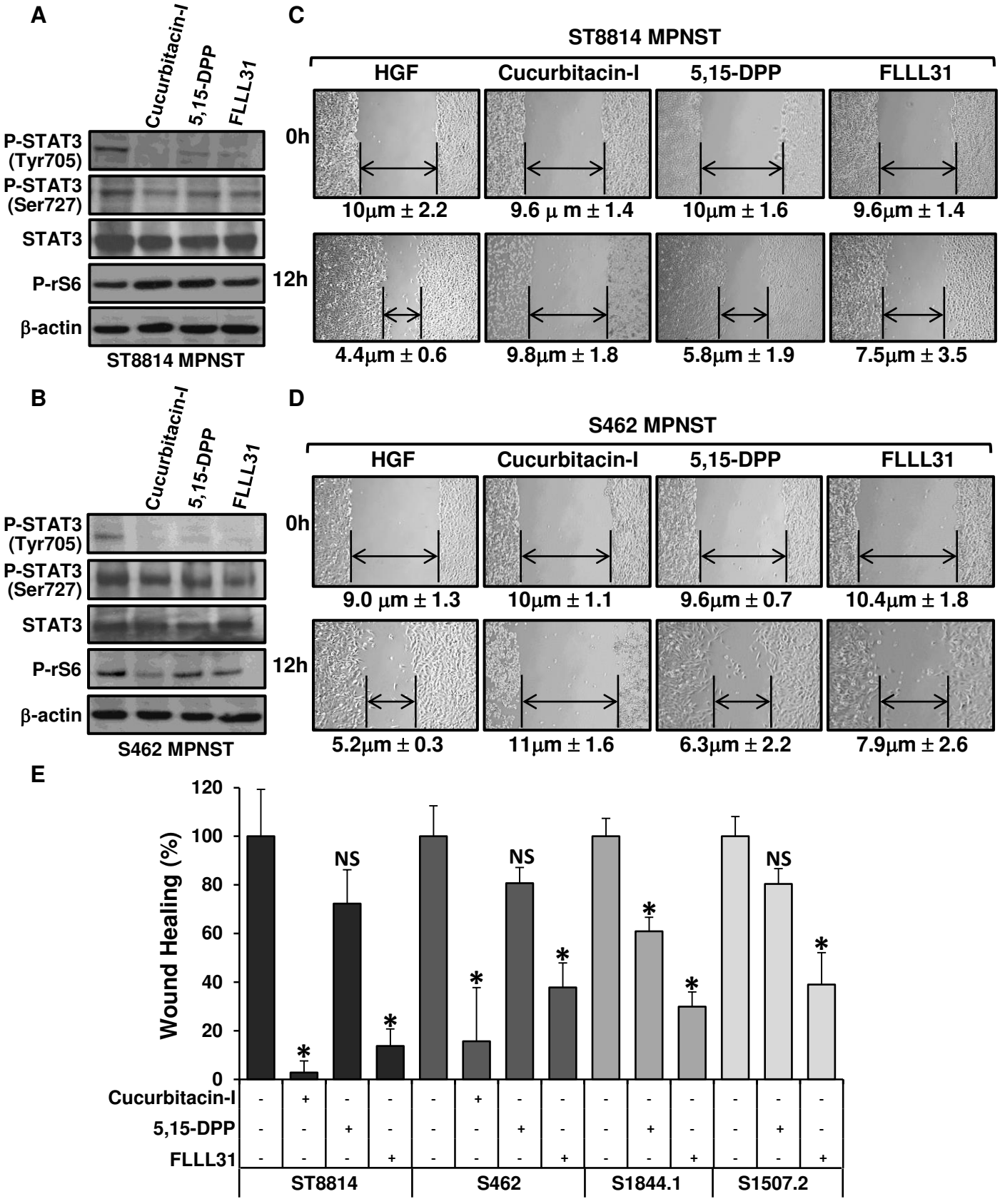
A
Cucurbitacin-I
5,15-DPP
FLLL31
P-STAT3 (Tyr705)
P-STAT3 (Ser727)
STAT3
P-rS6
β-actin
ST8814 MPNST
B
Cucurbitacin-I
5,15-DPP
FLLL31
P-STAT3 (Tyr705)
P-STAT3 (Ser727)
STAT3
P-rS6
β-actin
S462 MPNST
C
ST8814 MPNST
HGF
Cucurbitacin-I
5,15-DPP
FLLL31
0h
10μm ± 2.2
9.6 μ m ± 1.4
10μm ± 1.6
9.6μm ± 1.4
12h
4.4μm ± 0.6
9.8μm ± 1.8
5.8μm ± 1.9
7.5μm ± 3.5
D
S462 MPNST
HGF
Cucurbitacin-I
5,15-DPP
FLLL31
0h
9.0 μm ± 1.3
10μm ± 1.1
9.6μm ± 0.7
10.4μm ± 1.8
12h
5.2μm ± 0.3
11μm ± 1.6
6.3μm ± 2.2
7.9μm ± 2.6
E
Wound Healing (%)
120
100
80
60
40
20
0
NS
NS
NS
*
Cucurbitacin-I
5,15-DPP
FLLL31
ST8814
S462
S1844.1
S1507.2

Figure 5

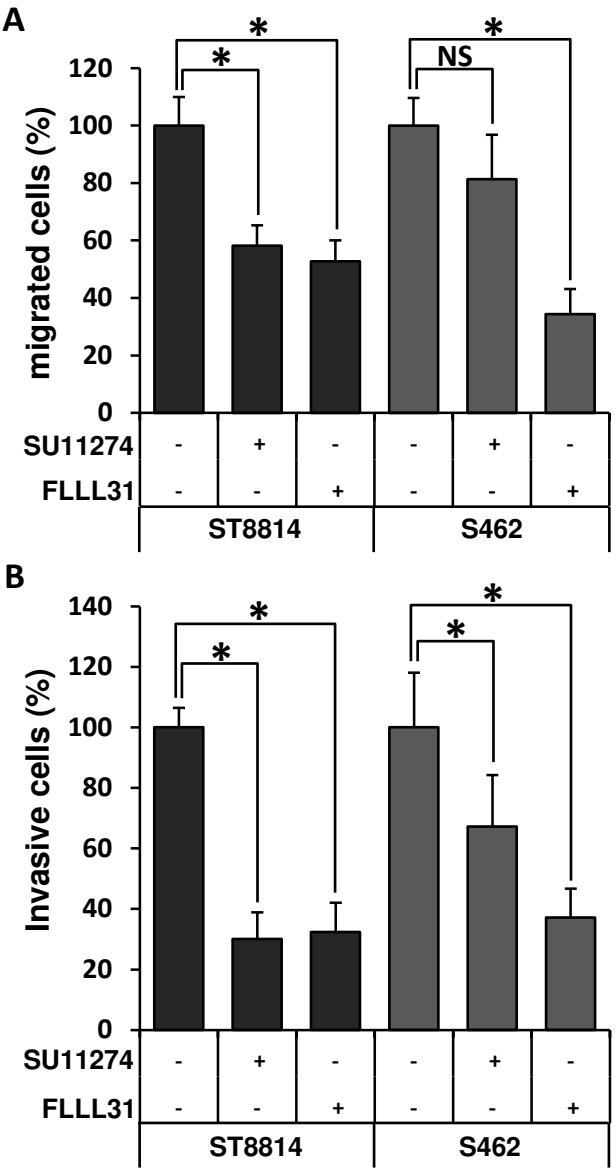
A
migrated cells (%)
120
100
80
60
40
20
0
*
*
NS
*
SU11274
FLLL31
ST8814
S462
B
Invasive cells (%)
140
120
100
80
60
40
20
0
*
*
*
SU11274
FLLL31
ST8814
S462

Figure 6

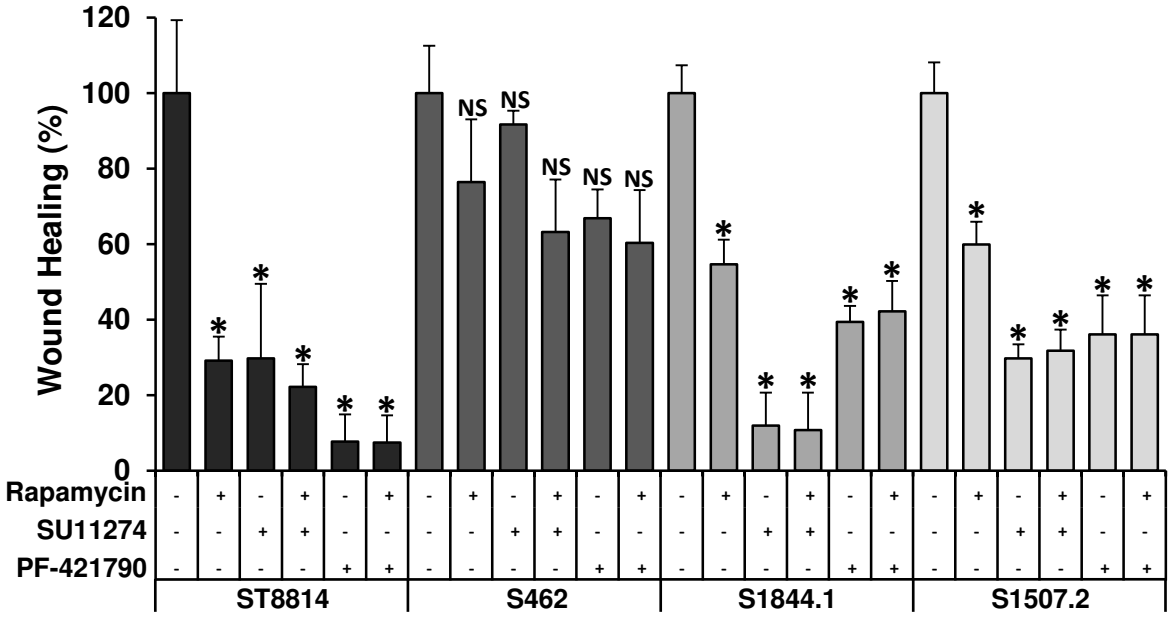
Wound Healing (%)
120
100
80
60
40
20
0
NS
Rapamycin
SU11274
PF-421790
ST8814
S462
S1844.1
S1507.2

Figure 7

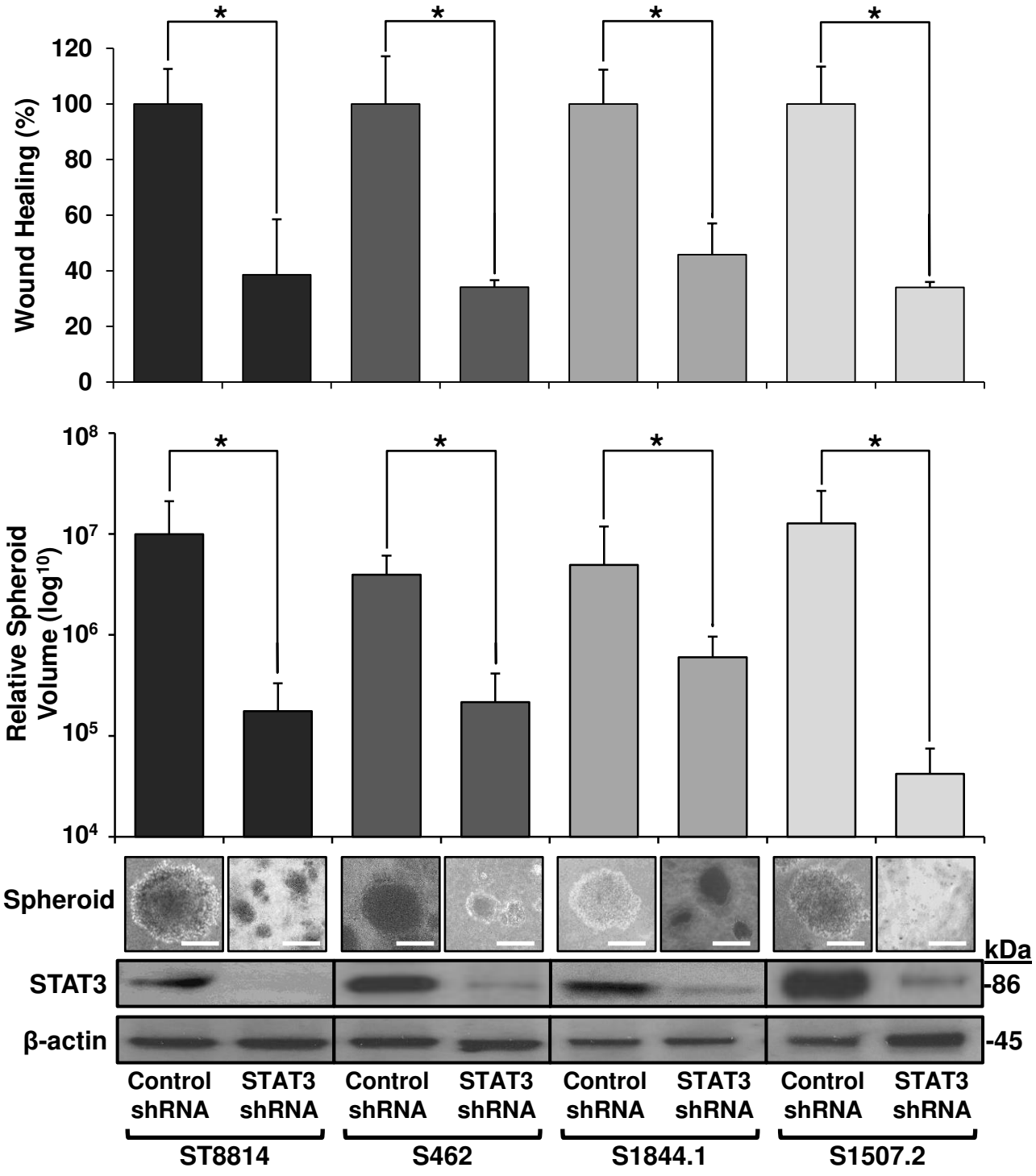
Wound Healing (%)
120
100
80
60
40
20
0
*
*
*
*
Relative Spheroid Volume (log10)
10^8
10^7
10^6
10^5
10^4
Spheroid
kDa
STAT3
-86
β-actin
-45
Control shRNA
STAT3 shRNA
ST8814
S462
S1844.1
S1507.2

Figure 8

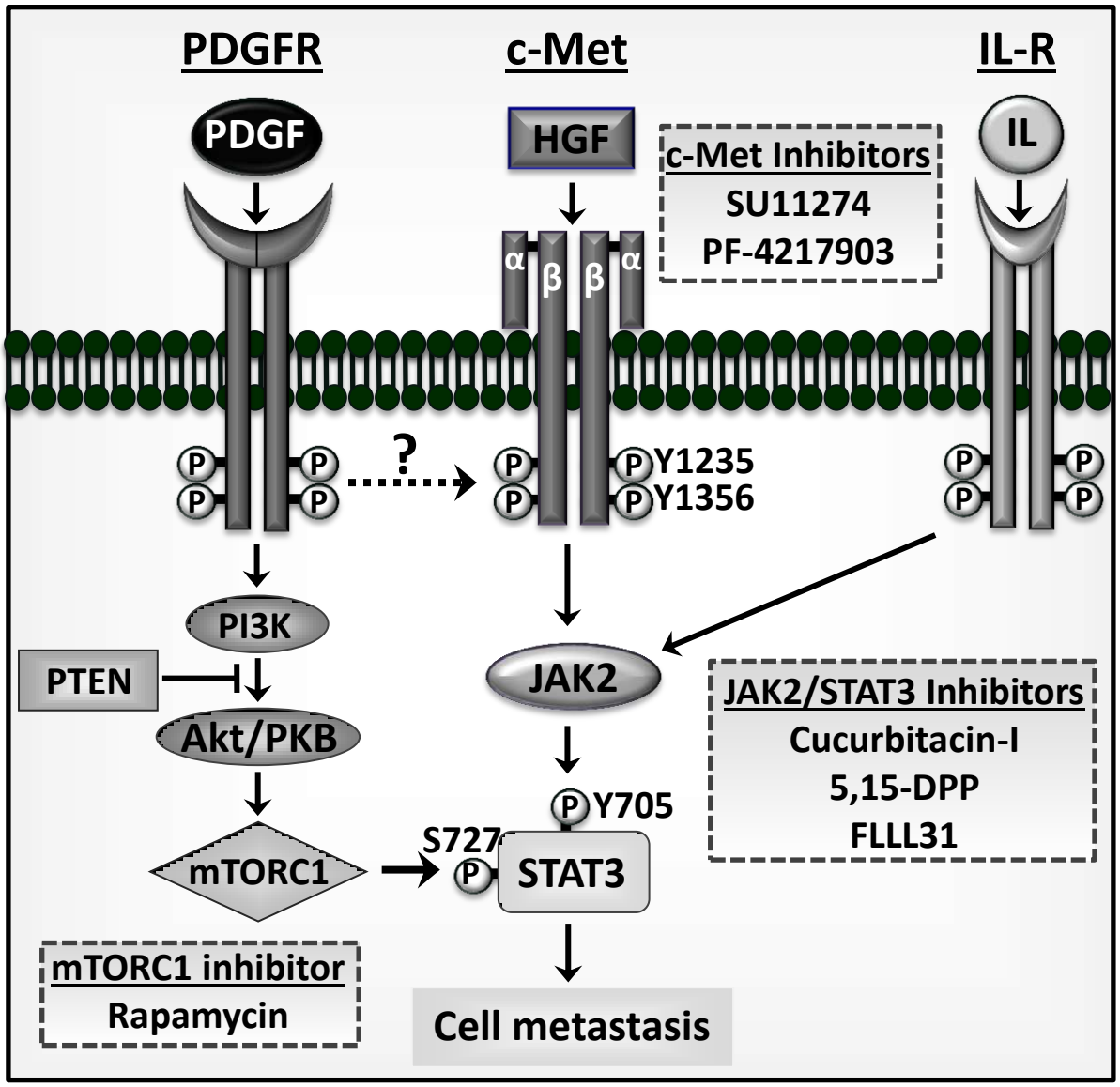
PDGFR
c-Met
IL-R
PDGF
HGF
IL
c-Met Inhibitors
SU11274
PF-4217903
α
β
β
α
P
?
Y1235
Y1356
PI3K
PTEN
Akt/PKB
JAK2
JAK2/STAT3 Inhibitors
Cucurbitacin-I
5,15-DPP
FLLL31
Y705
S727
mTORC1
STAT3
mTORC1 inhibitor
Rapamycin
Cell metastasis